ISSN 1064-2307, Journal of Computer and Systems Sciences International, 2019, Vol. 58, No. 2, pp. 286–296. © Pleiades Publishing, Ltd., 2019.
Russian Text © The Author(s), 2019, published in Izvestiya Akademii Nauk, Teoriya i Sistemy Upravleniya, 2019, No. 2, pp. 133–144.

CONTROL SYSTEMS OF MOVING OBJECTS

Reconstruction of a Spacecraft's Attitude Motion Using the Data on the Current Collected from Solar Panels

I. V. Belokonov[a], A. V. Kramlikh[a], I. A. Lomaka[a,*], and P. N. Nikolaev[a]

[a] *Korolev Samara State Aerospace University (National Research University), Samara, 443086 Russia*

**e-mail: igorlomaka63@gmail.com*

Received May 11, 2018; revised November 25, 2018; accepted November 26, 2018

Abstract—The problem of reconstructing a spacecraft's (SC's) attitude motion using measurements of a current from solar panels with the use of the differential evolution algorithm is considered; in this case the model of measurements takes into account the Earth-reflected light flux. The possibility of using the differential evolution algorithm and the model of measurements in the problem of the attitude motion reconstruction is substantiated by the example of the Aist SC. The application of this algorithm considerably simplifies the traditional technique for reconstructing the attitude motion.

DOI: 10.1134/S1064230719020047

INTRODUCTION

The attitude motion of a spacecraft (SC) is traditionally determined by the motion control system, which receives data from angular rate sensors, star trackers, local vertical detectors, Sun-direction sensors, etc. During the SC's flight, different off-nominal situations may arise onboard the SC, e.g., a full or partial failure of the measuring sensors of the motion control system; in this case the SC will make an uncontrolled rotation around the center of mass. In these cases, the SC's attitude motion is reconstructed using data from one/two operable measuring aids, e.g., using the geomagnetic field measurements [1], the angular rate measurements [2], the star tracker data [3], and the current values collected from panels of solar batteries (SBs) [4]. V.V. Sazonov substantially contributed to studying issues associated with the reconstruction of an SC's attitude motion [1–6].

This work also considers an SC's motion reconstruction by the readings of the current collected from the SB panels. However, in contrast to [4], to improve the adequacy of a model of measurements, a complicated model of measurements is used, which takes into account the Earth-reflected light flux. An important distinction of this work is also the application of the differential evolution algorithm (DEA), which only requires us to specify the domain of the solution's determination for the evaluated parameters instead of the traditional application of first-order algorithms sensitive to the initial approximation assignment and often resulting in the appearance of difficulties with the solution's convergence (e.g., the Gauss–Newton algorithm [5] and the Levenberg–Marquardt algorithm [6]).

Since its creation in 1995, the DEA [7] has developed a reputation as an efficient algorithm of global optimization and been applied to different problems, such as the N-body problem [8] and inverse problems [9, 10]. There are works comparing the DEA's efficiency with the efficiency of more traditional methods, such as the Powell and Nelder–Mead methods [9], the simulated annealing methodology [8], and the simple genetic algorithm [11].

With the use of the DEA, space-technology problems were solved; e.g., the optimal SC-flight trajectory was sought with its application in [12], while in [13] the optimal trajectories of motion of a robot-equipped manipulator for capturing space debris were sought using the DEA. In [14] the DEA was employed to find the SC's inertia moments in flight by applying the control actions using flywheels and attitude control thrusters to the SC. The solutions to the problem obtained using the DEA depend to a lesser degree on the initial conditions than those with the use of analogous algorithms. In this case, according to the authors, a more precise result is achieved, especially with a wider range of the possible value of the initial state vector [9].

The advantages of using the DEA in comparison to the given algorithms are as follows: first, the absence of the need to search for the initial approximation for the sought parameters. Secondly, there is no need for calculating partial derivatives of the function to be minimized, which allows avoiding the time-

consuming mathematical manipulations and provides the possibility to use more complicated mathematical models of attitude motion and models of measurements. Thirdly, the solution's accuracy is improved as there is no need to find partial derivatives numerically, and a search for the global extremum is provided in contrast to the first- and second-order methods, which frequently seek local extrema.

A disadvantage of the DEA application is the long time required for the calculations due to the large number of minimized-function calls.

This work presents the results of solving the problem of reconstructing an SC's attitude-motion based on the real data on current collection received from onboard the Aist-1 small spacecraft (SSC), which utilized magnetic coils to stabilize its motion (MagCom experiment) [15] during its flight in May 2013. This time interval was chosen to compare the reconstruction results obtained using the proposed approach with the results from [5].

Solving the problem of reconstructing attitude motion consists of the following stages:

(1) determining the parameters of the SC's center-of-mass motion on the required time interval (e.g., using the GNSS, processing TLE files [16, 17], or using the data from the flight control center) by integrating the equations of motion of the SC's center of mass with allowance for the second and fourth zonal harmonics of an expansion of the potential of the Earth's gravitational field;

(2) calculating the Sun's direction vector [18] and determining the shaded/sunlit portions of an orbit [19];

(3) applying the DEA to estimate the SC's state vector at the initial time moment.

1. UPDATED MODEL OF MEASUREMENTS

Due to the difficulty of taking into account the processes occurring in solar panels, we assume that a SB is a planar surface whose attitude is specified by a unit vector of the normal $\mathbf{n}$ in a bound coordinate system (BCS). The SB-generated current (I_d is the current from the direct solar radiation and I_{max} is the maximum value of the current from the panels; it is determined from telemetry; in this work $I_{max} = 0.95$ A) is assumed to be proportional to the cosine of the angle of the sunlight incident on the SB's photosensitive surface:

$$I_d = I_{max} \cos(\mathbf{n}, \mathbf{S}), \tag{1.1}$$

where $\mathbf{S}$ is the unit Sun-directed vector and $\cos(\mathbf{n}, \mathbf{S})$ is the cosine of the angle between the relevant vectors.

For sunbeams, the Earth optically is a very inhomogeneous and variable surface. In the photograph of the Earth from a great distance, a permanently-changing cloud cover can be seen, which almost completely hides the surface of the continents and seas. The visual brightness of different portions of the terrestrial globe varies within a wide range in both the visible and invisible regions of the spectrum. The reflected solar radiation is composed of the radiation reflected from the cloud cover, the radiation reflected from the underlying surface, and also the radiation scattered by the atmosphere.

An SC, moving in low orbits above the Earth surface, is irradiated at each moment of time only by some small area of its own, for which the local albedo may differ from the average planetary spherical albedo (Fig. 1).

The distinction of the local albedo from the average spherical albedo is caused not only by the fact that different portions of the Earth have a different reflectance but also the by fact that the reflectivity factor of most of the regions of the Earth's surface depend on the sunlight's incidence angle. At large angles, the glaring and mirroring surfaces reflect beams in a completely different way than the diffusing surfaces, even if under normal irradiation their reflectivity factors appear to be close. Experimental reflectance studies of snow, sand; soil, water, etc., have shown that the variation range of the albedo of different regions of the Earth's surface is very broad: from 0.03 for a forest to 0.9 for fresh snow [20].

Therefore, in contrast to [6], apart from allowance for current generation from direct sunlight described by model (1.1), in this work the current I_{ref} generated by the solar radiation reflected from the Earth is also taken into account:

$$I_{ref} = I_{max} A_{av} \varphi_2,$$

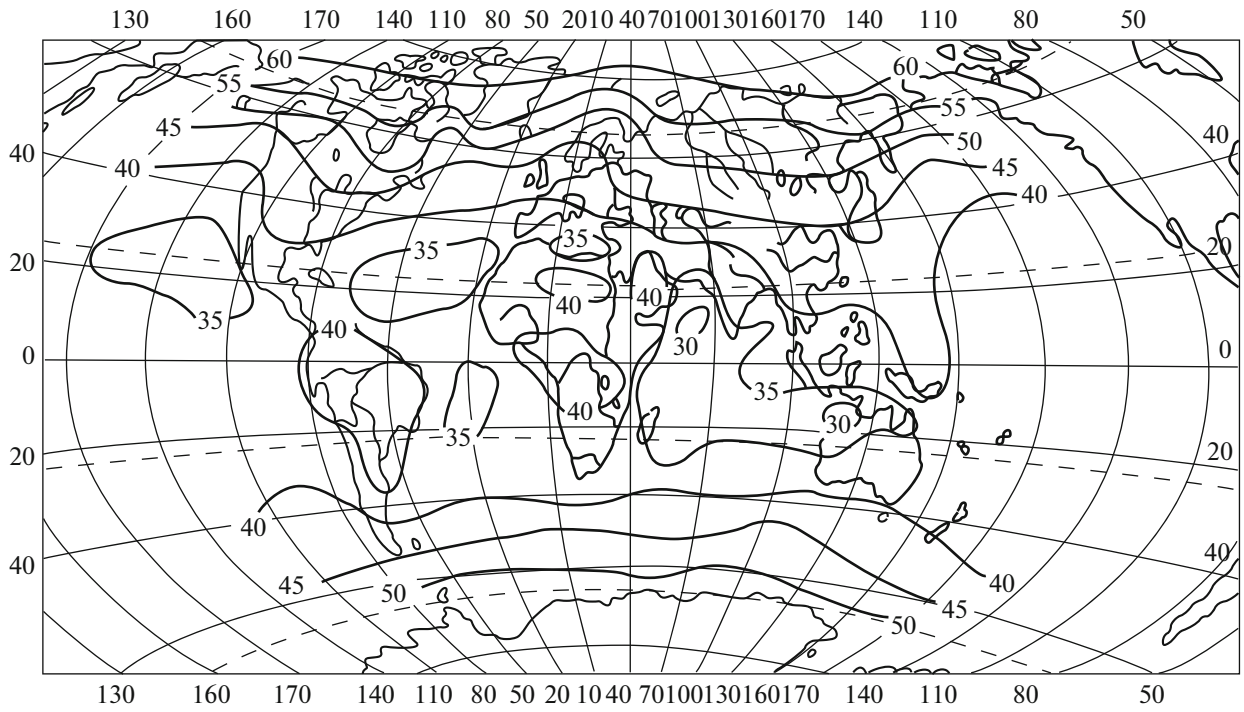

Fig. 1. Distribution of annual average albedo values over terrestrial globe.

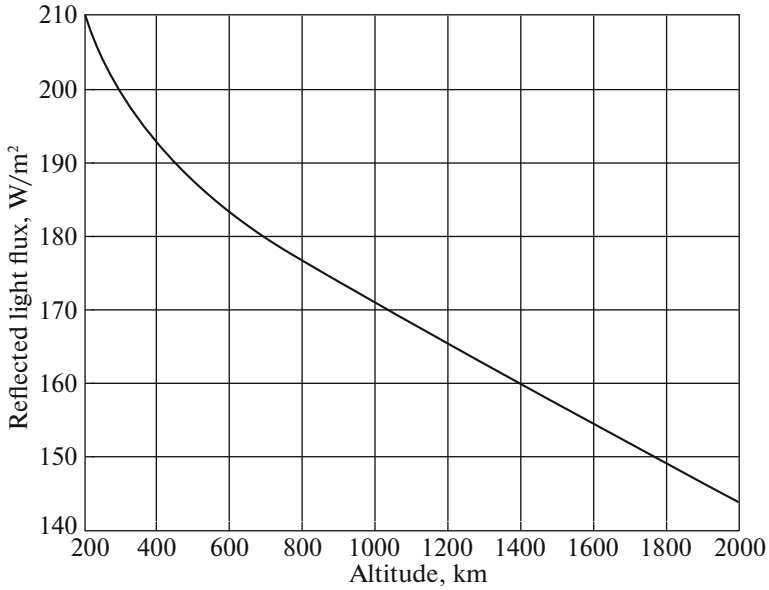

Fig. 2. Earth-reflected solar radiation as function of orbit altitude.

where A_{av} is the averaged value of the Earth's albedo and φ_2 is the combined angular coefficient [20]. Thus, the model of measurements in this work has the form

$$I = I_d + I_{ref}. \tag{1.2}$$

Works on studying the dependence of the Earth-reflected solar radiation on the orbit's altitude are known; this dependence is given in [21] (Fig. 2).

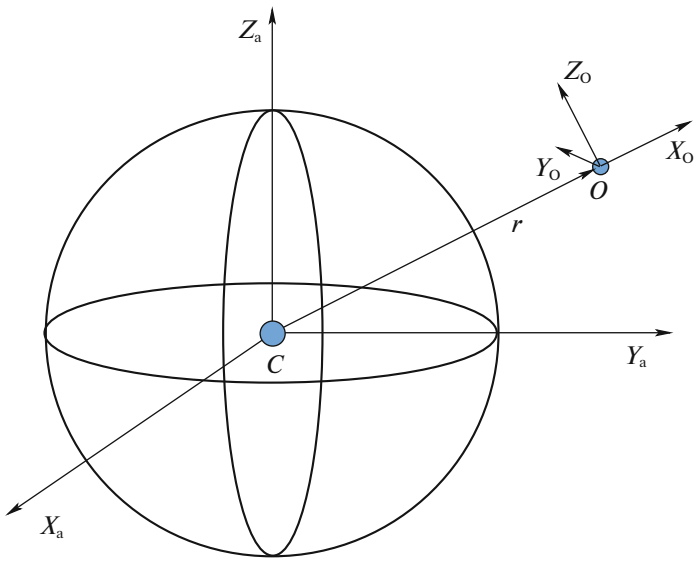

Fig. 3. Disposition of coordinate systems.

From Fig. 2 it can be seen that the fraction of the reflected radiation is on average 10 to 15% of the total light flux radiated by the Sun (1400 W/m^2).

2. PROBLEM FORMULATION FOR IDENTIFYING THE SC'S ATTITUDE-MOTION FROM THE DATA ON THE CURRENT COLLECTED FROM PANELS

For writing equations of the SC's motion around the center of mass (point O in Fig. 3) and the relations used in data processing, three right-hand Cartesian coordinate systems are introduced.

An SC's BCS is created by the principal central axes of inertia and has the designation of $OX_bY_bZ_b$. The geocentric absolute coordinate system (ACS) is denoted as $CX_aY_aZ_a$ with the origin at the Earth's center of mass (point C). The X_a axis points to the vernal equinox. The Z_a axis points to the Celestial North Pole. The Y_a axis complements the system to a right-handed one. The orbital coordinate system (OCS) is designated as $CX_oY_oZ_o$. The origin of the system is in the SC's center of mass. The X_o axis is directed along the SC's radius-vector. The Z_o axis is perpendicular to the orbit plane. The Y_o axis complements the system to a right-handed one.

The OCS is derived from the ACS using three consecutive turns: by the angle of the longitude of the ascending node Ω about the Z_a axis, by the angle of orbit inclination i about the new axis X_a', and by the argument of latitude u about the new axis Z_a''. The BCS's position with respect to the OCS is specified by three sequential rotations: through the angle of precession ψ about the Y_o axis, through the angle of attack α about the new axis Z_o', and through the angle of its own rotation φ about the new axis Y_o''.

The SC's rotational motion is described by Euler's dynamical equations (2.1) and kinematic equations (2.2) [5]. On the right-hand sides of Euler's dynamical equations, the gravity and dipole moments are taken into account. The equations of motion have the following form:

$$\begin{aligned}
\dot{\omega}_x &= \mu(\omega_y\omega_z - \nu a_{21}a_{31}) + p_2b_3 - p_3b_2,\\
\dot{\omega}_y &= \frac{1-\lambda}{1+\lambda\mu}(\omega_x\omega_z - \nu a_{31}a_{11}) + \frac{\lambda}{1+\lambda\mu}(p_3b_1 - p_1b_3),\\
\dot{\omega}_z &= -(1-\lambda+\lambda\mu)(\omega_x\omega_y - \nu a_{21}a_{11}) + \lambda(p_1b_2 - p_2b_1),
\end{aligned} \tag{2.1}$$

where $\lambda = I_x/I_z$ and $\mu = (I_y - I_z)/I_x$ are the dimensionless coefficients of inertia; $\nu = 3\mu_e/r^3$ is the coefficient of gravity moment; $p_1 = p\lambda\omega_x$, $p_2 = p(1+\lambda\mu)\omega_y$, and $p_3 = p\omega_z$ are the components of the satellite's magnetic dipole per I_x; p is the constant coefficient, showing that the SC's dipole moment is proportional

to the angular momentum vector; b_i is the vector component of the geomagnetic field induction (calculated by the IGRF model),

$$\frac{dq_0}{dt} = 0.5(-(\omega_x - \omega_{rx})q_1 - (\omega_y - \omega_{ry})q_2 - (\omega_z - \omega_{rz})q_3),$$

$$\frac{dq_1}{dt} = 0.5((\omega_x - \omega_{rx})q_0 + (\omega_z - \omega_{rz})q_2 - (\omega_y - \omega_{ry})q_3), \quad (2.2)$$

$$\frac{dq_2}{dt} = 0.5((\omega_y - \omega_{ry})q_0 + (\omega_x - \omega_{rx})q_3 - (\omega_z - \omega_{rz})q_1),$$

$$\frac{dq_3}{dt} = 0.5((\omega_z - \omega_{rz})q_0 + (\omega_y - \omega_{ry})q_1 - (\omega_x - \omega_{rx})q_2),$$

where $\boldsymbol{\omega}_r = A(q)\ [0\ \ 0\ \ \omega_{\text{orb}}]^{\text{T}}$ and ω_{orb} is the SC's orbital angular rate.

The matrix A of transferring from OCS to BCS is written as follows:

$$\begin{bmatrix} 1-2(q_2q_2+q_3q_3) & 2(q_1q_2+q_3q_0) & 2(q_1q_3-q_2q_0) \\ 2(q_1q_2-q_3q_0) & 1-2(q_1q_1+q_3q_3) & 2(q_2q_3+q_1q_0) \\ 2(q_1q_3+q_2q_0) & 2(q_2q_3-q_1q_0) & 1-2(q_1q_1+q_2q_2) \end{bmatrix}.$$

3. PROCEDURE FOR FINDING A NUMERICAL SOLUTION

Based on the least squares method, as an approximation of the SC's motion on the time interval, we assume a joint solution to systems (2.1) and (2.2), provided that by using them, the telemetry data on the current collected from the SB panels are best smoothed, i.e., the solution that ensures the minimum to the functional

$$J(b) = \sum_{i=1}^{6}\sum_{k=1}^{N_t}(I_{ik} - \hat{I}_{ik}(b))^2, \quad (3.1)$$

where $b = [\omega_x(t_0), \omega_y(t_0), \omega_z(t_0), \psi(t_0), \alpha(t_0), \varphi(t_0), A_{\text{av}}, \lambda, \mu, p]$ is the vector of the evaluated parameters, t_0 is the initial time moment of the measurements, i is the number of SBs (in the given case, six), and k is the number of current measurements received from each panel.

The quantities A_{av}, λ, and μ are the matching parameters. It should be noted that while approximating the attitude motion, computations are performed in quaternions; however, for the convenience of interpreting the result at the algorithm's input and output, the Euler angles are used.

The minimum to functional (3.1) is sought using the DEA [7] that includes the accomplishment of the following steps:

(1) specifying the initial array X consisting of N vectors b (N is constant at each iteration and is one of the DEA parameters); moreover, each element of vector b is generated at random within the required limits;

(2) generating a new array X_{new} of vectors b: for each vector b_i from the array X, three different vectors b_1, b_2, and b_3, whose indices do not coincide with the index of vector b_i, are selected at random and the so-called mutant vector is calculated by the formula $b_m = b_1 + F(b_2 - b_3)$, where F is the constant within the interval [0, 1], which is the DEA parameter;

(3) on the mutant vector b_m, a crossover operation is performed, which consists of the fact that some of its elements are replaced by the relevant elements of the initial vector b_i (each element is replaced at probability P, which is also another parameter of the DEA);

(4) if the obtained vector proves to be better than vector b_i, i.e., the value of the objective function decreases, $J(b_t) < J(b_i)$, then the vector b_i in the new array X_{new} is replaced by the new vector b_t (called a trial vector), otherwise, b_i is maintained;

(5) items 1–4 are repeated until the stop criterion is met.

The stop criterion depends on the problem to be solved. In this work the algorithm stops working as soon as the difference between the function values at the next and previous iterations becomes less than 0.001 A^2.

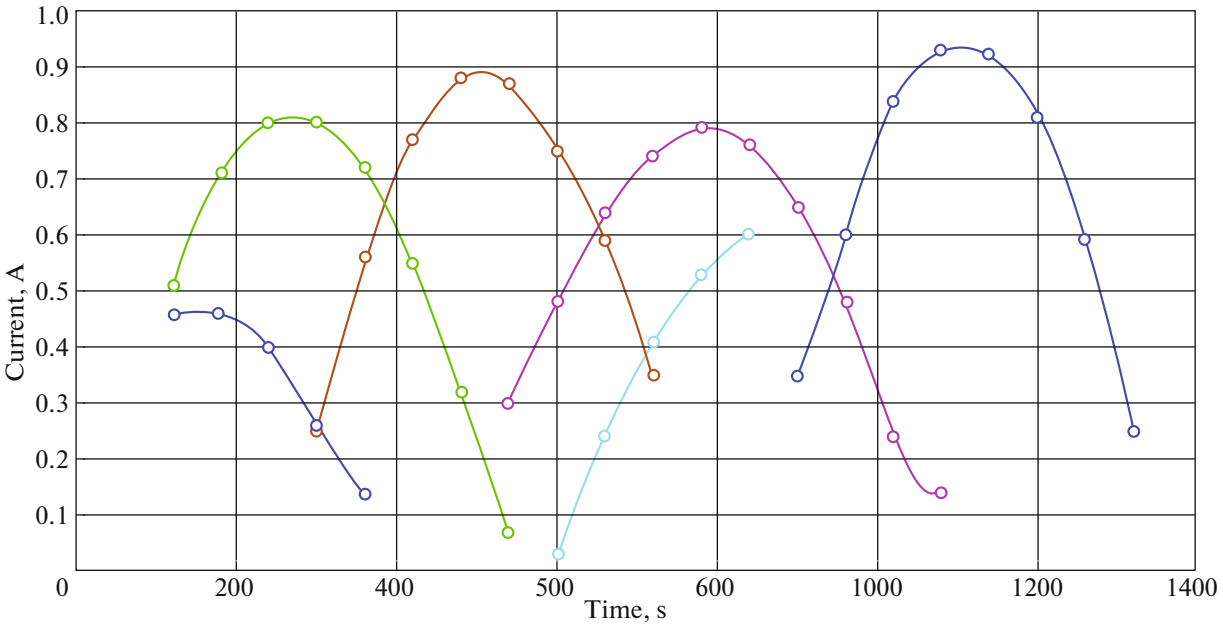

Fig. 4. Approximation of measurements (circles denote measured values of current; lines correspond to approximation data).

4. ESTIMATING THE EFFICIENCY OF USING THE DEA ON REAL MEASUREMENTS RECEIVED FROM THE AIST SSC

The Aist SSC has been developed by the TsSKB–Progress State Research-and-Production Space Rocket Centre jointly with the Samara State Aerospace University and is intended for scientific research. The satellite was launched on April 21, 2013, concurrently, by separating from the Bion M1 SC and moving along the near-circular orbit at an altitude of 570 km and an inclination of 54.9°. The orbital flight mode of the satellite is not oriented; the active lifetime is up to 3 years [5]. At this orbit altitude, the aerodynamic moment exerts a considerably smaller influence on the SC's rotational movement in comparison with the gravity moment; therefore in Eqs. (2.1), the influence of the atmosphere on the SC's motion is not taken into account.

The previous data processing on the current collection from the SB panels of the Aist SSC is the cubic-spline approximation of the measurements obtained from each of the six panels. The approximation is necessary for recalculating the measurements to the time moments of the calculation of the attitude motion. The current measurements were conducted with a period of 60 to 61 s; therefore, the variation in the current collection is approximated with a step of 10 s. The chosen time step of approximation allows Eqs. (2.1) and (2.2) to be integrated with the required accuracy. The results of smoothing are presented in Fig. 4. The measurements are obtained on the time interval from 21:13 DMT March 16, 2013 to 22:21 DMT March 16, 2013.

To solve a problem of reconstructing the attitude motion for the Aist SSC, the following DEA parameters were used (these parameters are traditionally advised for this algorithm): $N = 140$; $F = 0.5$; and $P = 0.9$. The results of the algorithm's operation are given in Fig. 5. A search for the evaluated parameters is implemented in the following ranges: the initial attitude angles ($\psi(t_0)$, $\alpha(t_0)$, and $\varphi(t_0)$) were determined within the range from 0 to 2π radians; the initial angular rates ($\omega_x(t_0)$, $\omega_y(t_0)$, and $\omega_z(t_0)$), within the range of ± 2 deg/s; the dimensionless coefficients λ and μ, within the ranges from 0.7 to 1.5 and from -0.5 to 0.5, respectively; the average Earth's albedo, within the range from 0 to 1; and limitations on the coefficient of dipole moment p were not imposed. As a result of the algorithm's operation, the following estimates of the sought parameters are obtained (Table 1): the approximation of current measurements by the mathematical model is presented in Fig. 5 and the dependence of the value of functional (3.1) on the iteration number is given in Fig. 6.

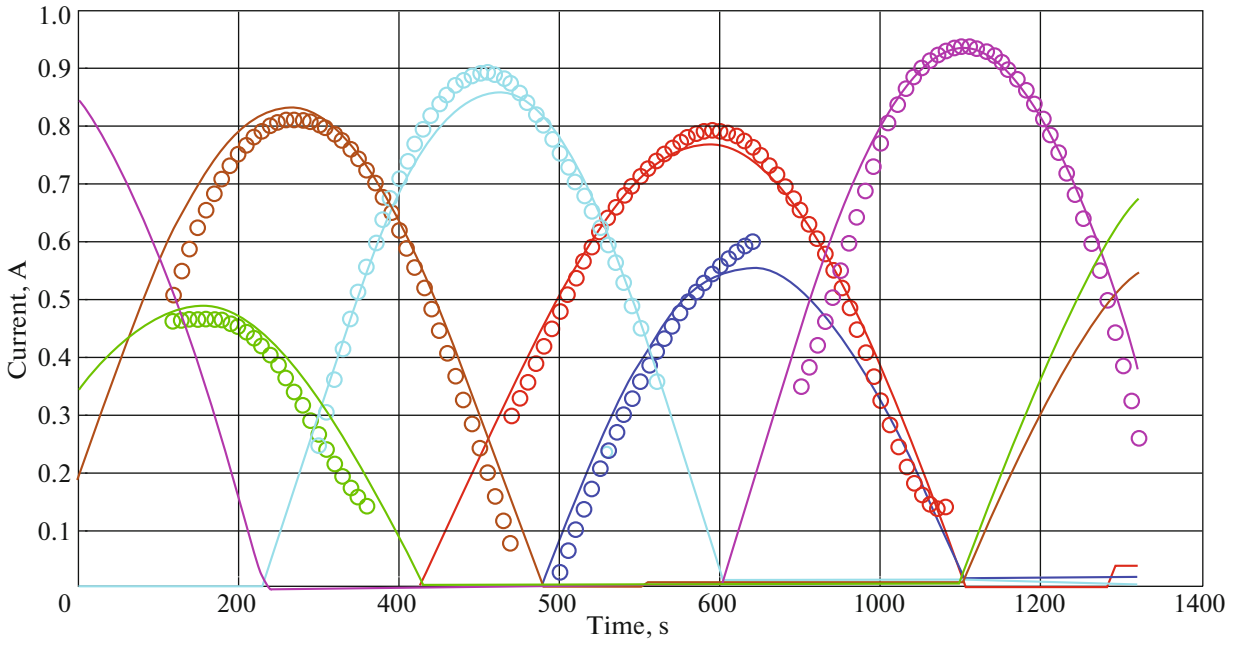

Fig. 5. Approximation of measurements (circles denote smoothed values of current; lines correspond to approximation by mathematical model (1.2)).

To estimate the approximation accuracy, the following formula of the standard deviation was used [6]:

$$\sigma = \sqrt{\frac{J(b_k)}{N-8}}, \tag{4.1}$$

where $J(b_k)$ is the functional value at the last iteration; in this problem, $J(b_k) = 0.2515$ A^2, $N = 234$, and $\sigma = 0.04$ A.

We define the relative error of approximation of the current values as $\sigma_{rel} = (\sigma/I_{max}) \times 100\%$. For the solution obtained in this work, $\sigma_{rel} = 4\%$, while the result in the analogous problem solved in [6] is similar in accuracy, $\sigma_{rel} = 3.8\%$, which testifies to the fact that the given solution is valid.

According to Fig. 2 [21], the value of the Earth-reflected solar radiation at the Aist SSC flight altitude is on the order of 180 W/m^2. Taking into account that the value of the direct solar radiation is 1400 W/m^2, the average albedo value is $A_{av} = 180/1400 = 0.128$, which is close to the estimate obtained in this work: $A_{av} = 0.102$.

Table 1. Results of algorithm operation

Quantity	Value
$\omega_x(t_0)$, rad/s	0.0041
$\omega_y(t_0)$, rad/s	0.002
$\omega_z(t_0)$, rad/s	–0.0026
$\psi(t_0)$, rad	5.448
$\alpha(t_0)$, rad	1.3
$\varphi(t_0)$, rad	3.93
A_{av}	0.102
λ	0.832
μ	0.214
p, C/kg	-18×10^9

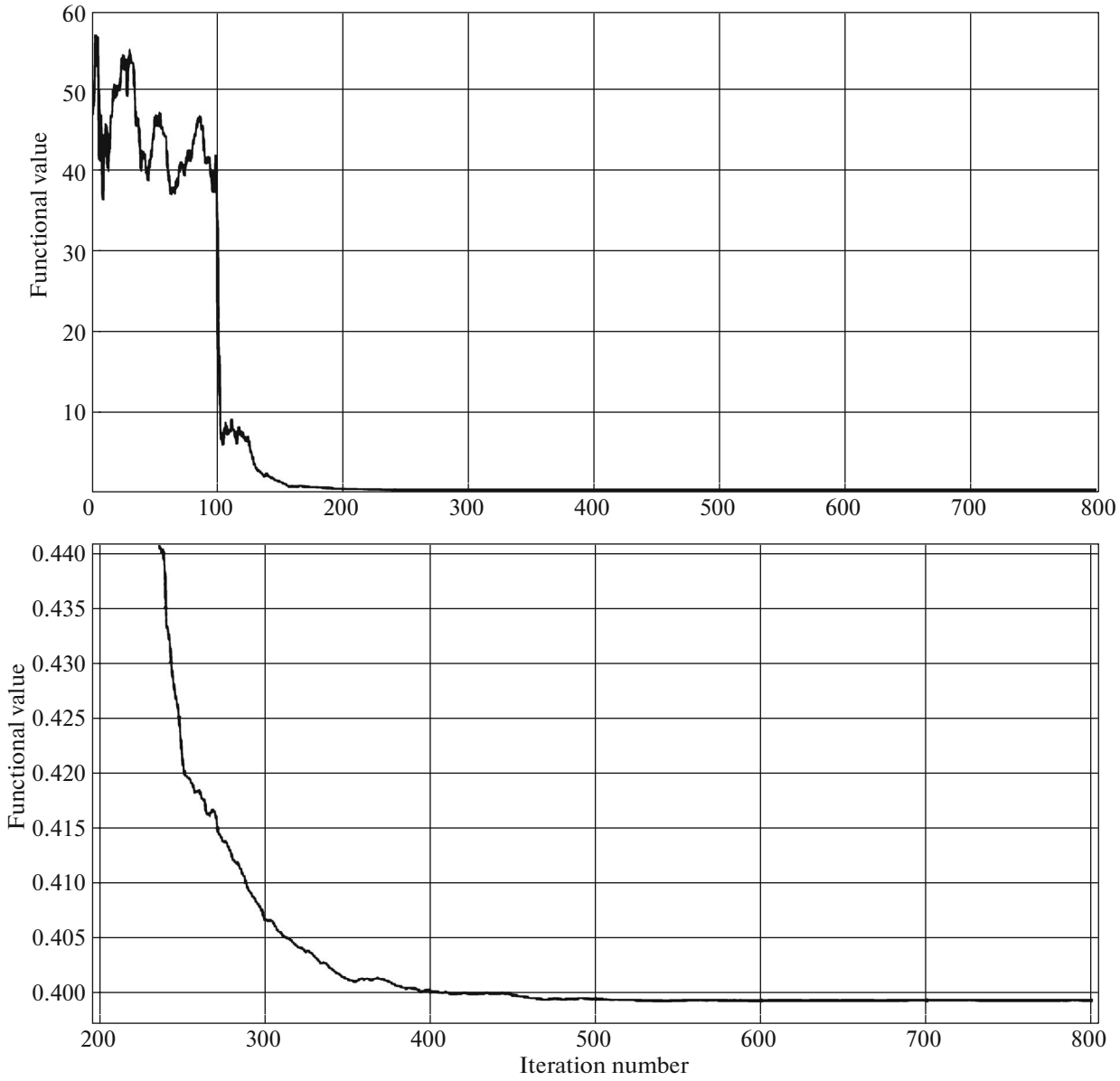

Fig. 6. Dependence of value of functional (3.1) on iteration number.

We note that the coefficients of inertia determined in this work, $\lambda = 0.832$ and $\mu = 0.214$, differ considerably from the relevant coefficients (we denote them as λ_5 and μ_5), given in [5]. This is explained by the fact that the BCS [5] in which the Aist SSC's moments of inertia are defined differs from the BCS of this work. Let us set up a correspondence between the moments of inertia in our work and in [5]. For this purpose we arrange the moments of inertia in their ascending order. From the analysis of the λ and μ values of [5], the relation $I_2 > I_1 > I_3$ follows, while in this work, $I_y > I_z > I_x$. Since the subject of research in both works is the same SC, then the following correspondences can be constructed between the moments of inertia: $I_y \leftrightarrow I_2$, $I_z \leftrightarrow I_1$, and $I_x \leftrightarrow I_3$. We recalculate the obtained λ and μ with allowance for the relations $\lambda_1 = 1/\lambda = 1.202$ and $\mu_1 = (1 - \lambda + \lambda\mu) = 0.346$. The derived coefficient values correspond to the data given in [5].

Thus, a conclusion on the operational suitability of the DEA and the mathematical model of the current collection measurements for determining the parameters of the SC's rotational motion can be drawn. The found estimate of the magnitude of the Aist SSC's angular rotation rate at the time moment of 21:13 DMT on 16 May, 2013, $|\boldsymbol{\omega}| = 0.346$ deg/s, is close to the value of $|\boldsymbol{\omega}| = 0.338$ deg/s from [5] for the same

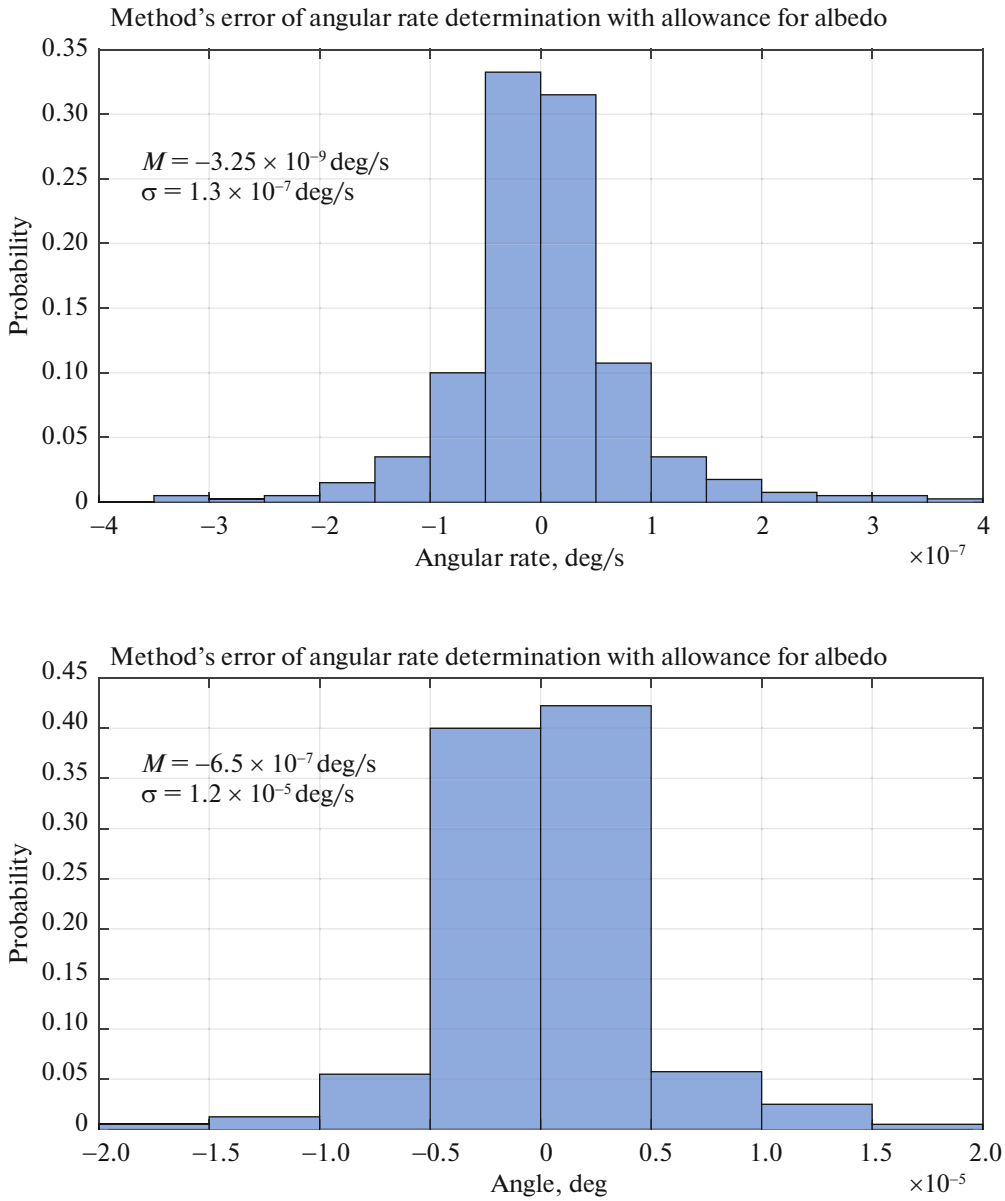

Fig. 7. Distribution of probability of errors of reconstruction of attitude motion parameters with allowance for Earth's albedo.

time moment, which also confirms the correctness of the result obtained and the possibility of applying the DEA to solve problems that reconstruct the attitude motion.

5. ESTIMATION OF THE EFFECT OF TAKING THE EARTH'S ALBEDO INTO ACCOUNT IN RECONSTRUCTING THE ATTITUDE MOTION PROBLEM

To estimate the influence of the allowance for the Earth's albedo, a statistical simulation of the problem solution was carried out. The simulation occurred as follows:

(1) In a random way, 400 options of the initial conditions of attitude motion ($\omega_x(t_0)$, $\omega_y(t_0)$, $\omega_z(t_0)$, $\psi(t_0)$, $\alpha(t_0)$, $\varphi(t_0)$) were generated on the assumption of the equiprobable law of their distribution. It was believed that $|\boldsymbol{\omega}| \le 1$ deg/s, $\psi(t_0)$ and $\varphi(t_0)$ lie in the range from 0° to 360°, while $\alpha(t_0)$ lies from 0° to 180°.

(2) For each option of the initial conditions, the current measurements were simulated, which took into account the influence of the Earth's albedo, according to Eq. (1.2), on the assumption of the absence of noise in the measurements.

(3) Each measurement array was used to reconstruct the initial conditions of the attitude motion twice: in the first case the reconstruction algorithm took the Earth's albedo into account, while in the second case, it did not take it into account.

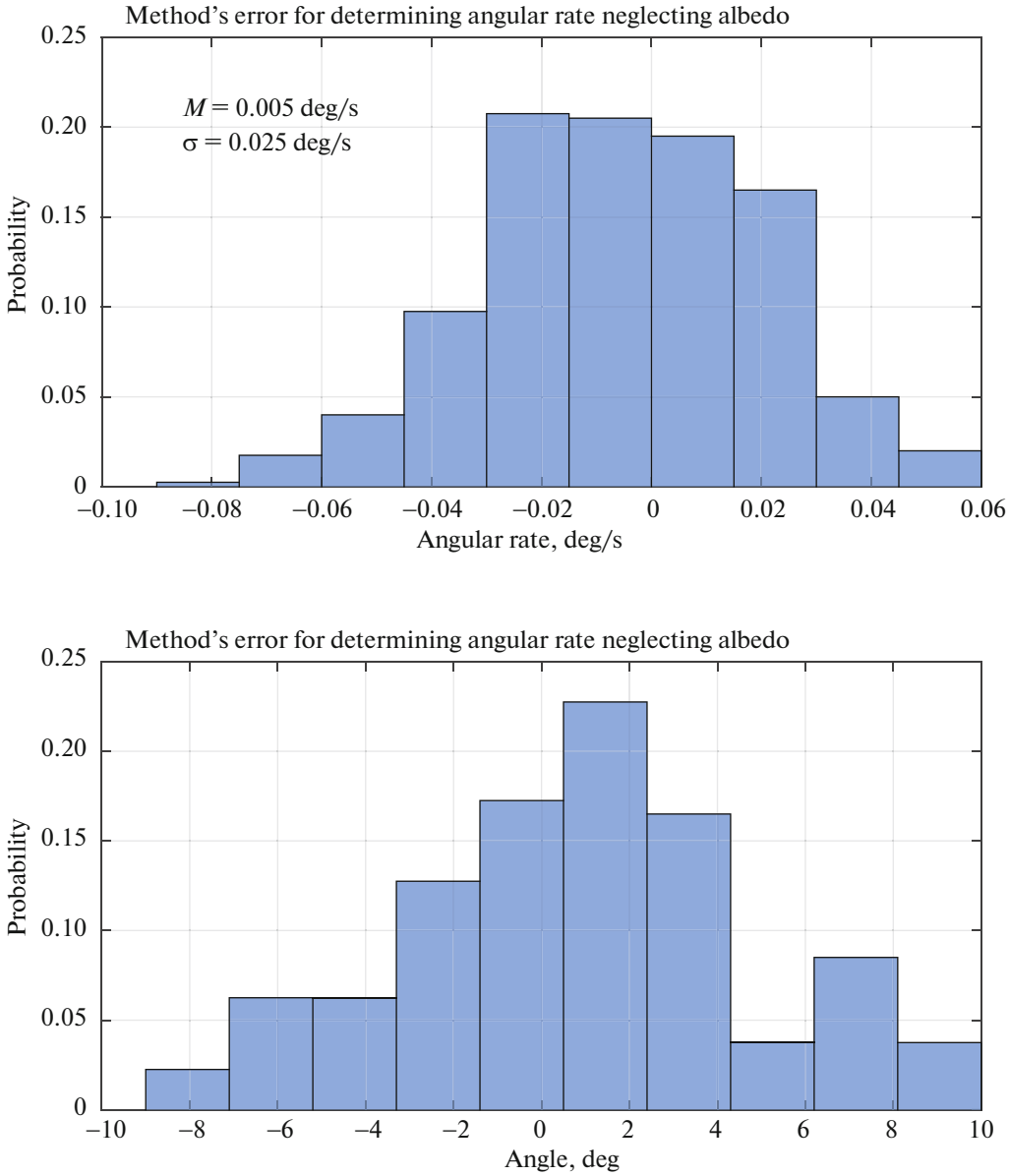

Fig. 8. Distribution of probability of errors of reconstructing attitude motion parameters neglecting Earth's albedo.

(4) The results of solving the problem in both cases were compared with the initial conditions which were used to simulate the measurements. As a result, the errors of the method of the algorithm for reconstructing the attitude motion were obtained and the influence of the allowance for the Earth's albedo on the results of reconstructing the attitude motion was determined.

The simulation results are given in Figs. 7 and 8, where the following designations are used: M is the mathematical expectation and σ is the standard deviation. According to the results obtained, neglecting the Earth-reflected radiation leads to errors in determining the attitude on the order of 12° (3σ), and the angular rate, on the order of 0.075 deg/s (3σ).

CONCLUSIONS

The algorithm proposed in this work makes it possible not only to reconstruct the SC's attitude motion from the current collection measurements but also to estimate the moments of inertia with sufficient accuracy, which is confirmed by the example of the Aist SSA.

The results obtained agree with the SC's technical documentation data and are compatible with [5]. The estimate of the Earth's average albedo found from the results of processing the current collection

readings is in agreement with [21]. The motivation for the use of the reflected solar radiation in the problem of determining the SC's rotational motion is substantiated. The contribution of errors, which arise due to neglecting the reflected solar radiation, to reconstructing the attitude motion is estimated. As there is no need to specify a "good" initial approximation, the utilized DEA has a large domain of convergence and can be applied to identify objects whose parameters are unknown.

ACKNOWLEDGMENTS

This work was supported by the Russian Science Foundation (project no. 17-79-20215).

REFERENCES

1. V. I. Abrashkin, V. L. Balakin, I. V. Belokonov, K. E. Voronov, A. S. Zaitsev, V. V. Ivanov, A. E. Kazakova, V. V. Sazonov, and N. D. Semkin, "Determination of the spacecraft Foton-12 attitude motion on measurements of the earth magnetic field," KIAM Preprint No. 60 (Keldysh Inst. Appl. Math., Moscow, 2000).
2. M. Yu. Belyaev, O. N. Volkov, M. I. Monakhov, and V. V. Sazonov, "Accuracy estimation of the technique for reconstructing the spacecraft attitude motion by measurements of its angular rate and Earth magnetic field strength," KIAM Preprint No. 4 (Keldysh Inst. Appl. Math., Moscow, 2016).
3. G. A. Avanesov, R. V. Bessonov, A. N. Kurkina, A. V. Nikitin, and V. V. Sazonov, "Determination of a spacecraft attitude motion by measurements of four star sensors," KIAM Preprint No. 57 (Keldysh Inst. Appl. Math., Moscow, 2016).
4. M. Yu. Belyaev, T. V. Matveeva, M. I. Monakhov, V. V. Sazonov, and V. V. Tsvetkov, "Reconstruction of spacecraft progress attitude motion by measurements of their angular rate and electric current from solar batteries," KIAM Preprint No. 39 (Keldysh Inst. Appl. Math., Moscow, 2012).
5. V. I. Abrashkin, K. E. Voronov, A. V. Piyakov, Yu. Ya. Puzin, V. V. Sazonov, N. D. Semkin, A. S. Filippov, and S. Yu. Chebukov, "Determination of the spacecraft aist attitude motion on measurements of the Earth magnetic field," KIAM Preprint No. 17 (Keldysh Inst. Appl. Math., Moscow, 2014).
6. A. A. Davydov and V. V. Sazonov, "Reconstruction of attitude motion of the small spacecraft by measurements of the current from solar arrays," KIAM Preprint No. 32 (Keldysh Inst. Appl. Math., Moscow, 2009).
7. R. Storn and K. Price, *Differential Evolution—A Simple and Efficient Adaptive Scheme for Global Optimization over Continuous Spaces* (Int. Comput. Science Inst., Berkeley, 1995).
8. N. Chakraborti, "Genetic algorithms and related techniques for optimizing Si-H clusters: a merit analysis for differential evolution," in *Differential Evolution, Natural Computing Series* (Springer, Berlin, 2005), pp. 313–326.
9. B. Růžek and M. Kvasnička, "Determination of the earthquake hypocenter: a challenge for the differential evolution algorithm," in *Differential Evolution, Natural Computing Series* (Springer, Berlin, 2005), pp. 379–391.
10. M. Wormington, K. M. Matney, and D. K. Bowen, "Application of differential evolution to the analysis of X-ray reflectivity data," in *Differential Evolution, Natural Computing Series* (Springer, Berlin, 2005), pp. 463–478.
11. R. Joshi and A. C. Sanderson, "Minimal representation multi-sensor fusion using differential evolution," in *Differential Evolution, Natural Computing Series* (Springer, Berlin, 2005), pp. 353–377.
12. W. Changqing, X. Rui, Z. Shengying, and C. Pingyuan, "Time-optimal spacecraft attitude maneuver path planning under boundary," Acta Astronaut., No. 4, 128–137 (2017).
13. W. Mingming, L. Jianjun, F. Jing, and Y. Jianping, "Optimal trajectory planning of free-floating space manipulator using differential evolution algorithm," Adv. Space Res., No. 3, 1525–1536 (2018).
14. S. Mingliang, C. Xinlong, and L. Shunli, "Identification of mass characteristic parameters for spacecraft based on differential evolution algorithm," in *Proceedings of the 5th International Conference on Instrumentation and Measurement, Computer, Communication and Control IMCCC, Qinhuangdao, 2015.*
15. A. N. Kirilin, R. N. Akhmetov, V. I. Abrashkin, E. V. Shakhmatov, V. A. Soifer, S. I. Tkachenko, A. B. Prokofiev, N. R. Stratilatov, V. V. Salmin, N. D. Semkin, and I. S. Tkachenko, "Design, testing and operation of aist small satellites," in *Proceedings of the 7th International Conference on Recent Advances in Space Technologies, Istanbul, 2015,* pp. 819–823.
16. F. R. Hoots and R. L. Roehrich, "Models for propagation of NORAD element sets," Spacetrack Report No. 3 (USA, 1988).
17. A. I. Manturov, *Mechanics of Spacecraft Motion Control* (Samar. Gos. Aviats. Univ., Samara, 2003), pp. 38, 39 [in Russian].
18. The Forecast of the Spacecraft Orbital Motion. Numerical Model 2007. http://vadimchazov.narod.ru/text_pdf/comalg.pdf.
19. V. K. Srivastava, A. M. Pitchaimani, and B. S. Chandrasekhar, "Eclipse prediction methods for LEO satellites with cylindrical and cone geometries: a comparative study of ECSM and ESCM to IRS satellites," Astron. Comput. **2**, 88–96 (2013).
20. L. V. Kozlov, M. D. Nusinov, and A. I. Akishin, *Simulation of the Thermal Regimes of the Spacecraft and its Environment* (Mashinostroenie, Moscow, 1971) [in Russian].
21. D. Bhanderi and T. Bak, "Modeling Earth albedo for satellites in Earth orbit," in *Proceedings of the AIAA Conference on Guidance, Navigation and Control, San Francisco, 2005.*

Translated by M. Samokhina